HHS Public Access

Author manuscript

Osteoarthritis Cartilage. Author manuscript; available in PMC 2021 March 01.

Published in final edited form as:

Osteoarthritis Cartilage. 2020 March ; 28(3): 375–382. doi:10.1016/j.joca.2019.12.006.

MOLECULAR AND MACROMOLECULAR DIFFUSION IN HUMAN MENISCUS: RELATIONSHIPS WITH TISSUE STRUCTURE AND COMPOSITION

Francesco Travascio[1,2,*], **Floriane Devaux**[3], **Mallory Volz**[3], **Alicia R. Jackson**[3,*]

[1]Department of Industrial Engineering, University of Miami, Coral Gables, FL

[2]Max Biedermann Institute for Biomechanics at Mount Sinai Medical Center, Miami Beach, FL

[3]Department of Biomedical Engineering, University of Miami, Coral Gables, FL

Abstract

Objective: To date, the pathophysiology of the meniscus has not been fully elucidated. Due to the tissue's limited vascularization, nutrients and other molecular signals spread through the extracellular matrix via diffusion or convection (interstitial fluid flow). Understanding transport mechanisms is crucial to elucidating meniscal pathophysiology, and to designing treatments for repair and restoration of the tissue. Similar to other fibrocartilaginous structures, meniscal morphology and composition may affect its diffusive properties. The objective of this study was to investigate the role of solute size, and tissue structure and composition on molecular diffusion in meniscus tissue.

Design: Using a custom FRAP technique developed in our lab, we measured the direction-dependent diffusivity in human meniscus of six different molecular probes of size ranging from ~300Da to 150,000Da. Diffusivity measurements were related to sample water content. SEM images were used to investigate collagen structure in relation to transport mechanisms.

Results: Diffusivity was anisotropic, being significantly faster in the direction parallel to collagen fibers when compared the orthogonal direction. This was likely due to the unique structural organization of the tissue presenting pores aligned with the fibers, as observed in SEM images. Diffusion coefficients decreased as the molecular size increased, following the Ogston model. No significant correlations were found among diffusion coefficients and water content of the tissue.

[*]Corresponding authors: Dr. Francesco Travascio, Associate Professor, College of Engineering, University of Miami, 1251 Memorial Drive, MEB 276, Coral Gables, FL 33146, USA, Telephone: +1-(305)-284-2371, Fax: +1-(305)-284-4040, f.travascio@miami.edu, Dr. Alicia R. Jackson, Associate Professor, College of Engineering, University of Miami, 1251 Memorial Drive, MEA 219, Coral Gables, FL 33146, USA, Telephone: +1-(305)-284-2135, Fax: +1-(305)-284-4040, a.jackson2@miami.edu.

AUTHORS CONTRIBUTION

FT conducted the experiments, analyzed the data and prepared the manuscript. FD and MV participated to experiments and data analysis, and reviewed the manuscript. AJ participated to data analysis and prepared the manuscript.

Conclusions: This study provides new knowledge on the mechanisms of molecular transport in meniscal tissue. The reported results can be leveraged to further investigate tissue pathophysiology and to design treatments for tissue restoration or replacement.

INTRODUCTION

The fibrocartilaginous meniscus plays a crucial role in the functioning of the knee joint, bearing 45–75% of the total load on the knee, as well as maintaining congruency and lubrication in the joint [1]. Osteoarthritis (OA) is rapidly becoming a leading cause of disability in the aging population, affecting 1 in 2 adults and costing more than $100 billion annually in the US alone [2]. Moreover, the knee joint is one of the most susceptible joints to OA changes. The degeneration of the meniscus, which may include wearing and laceration, affects approximately 35% of the population [3]. This condition is associated with the initiation and progression of OA in the knee, although the causative nature is not well understood.

A distinct feature of the meniscus is its lack of full vascularization. In the mature tissue, blood vessels are found in only the outer 10–30% of the tissue (called the red zone), while the remaining inner portion is avascular (called the white zone) [4]. As a result, the white zone and its resident cells must rely on transport from the outer vasculature to meet their metabolic needs (i.e., delivery of nutrients and removal of metabolic wastes). In addition, other important molecules, such as growth factors, enzymes, and cytokines, must also be transported through the tissue to reach cells in the avascular zone. This occurs either by diffusion or by convective transport due to fluid flow during tissue compression. It has been shown that, unlike lesions in the vascularized region, those in the white zone are not capable of self-repair; in fact, proximity to blood vessels is generally considered to be the best predictor of meniscus healing [5, 6]. In order to better understand tissue healing response and pathophysiology, knowledge of tissue transport properties is essential. Only few previous studies have investigated solute transport properties in meniscus tissues [7, 8]. In general, these studies are limited to small solutes and have been measured in animal (e.g., bovine, porcine) tissues. It is generally understood that solute diffusivity is inversely proportional to solute size in cartilaginous tissues [9], although the particular quantitative relationship for meniscus is not known.

In addition to the unique vascularization of the tissue, the meniscus is also characterized by a particular collagen fiber organization in its extracellular matrix (ECM). While collagen fibers on the surface of the tissue are randomly organized, those in the deeper core of the meniscus are circumferentially oriented [10]. This ECM structure has been studied extensively with regard to the anisotropic mechanical properties of the meniscus under compression, tension, and shear loading conditions [11–21]. However, diffusion of solutes through the ECM is also highly dependent upon the tissue structure. Previous studies have investigated the anisotropic diffusion coefficient of small solutes (i.e., glucose, fluorescein) in animal meniscus tissues [7, 8]. These studies found that diffusion occurs more rapidly along the direction of collagen fiber bundles in the tissue. However, to our knowledge, no previous study has investigated the anisotropic nature of molecular diffusion in human meniscus tissues, nor has a variety of solute sizes been examined.

Besides gaining insight into tissue pathophysiology, knowledge of molecular transport behavior in meniscus tissues is also critical for developing new strategies to treat and/or repair the tissue. For example, when designing engineered tissue constructs for tissue repair, consideration of transport properties is important given that essential solutes (e.g., nutrients, cytokines, growth factors, etc.) must be able to traffic through the scaffold to reach cells both inside the scaffold and in the surrounding the tissue (e.g., in the case of moving from the vascular to avascular regions). Moreover, quantitative information on solute transport is critical for the development of computational models of the meniscus, which can be employed to understand and predict tissue behavior *in vivo*, and also to derive new treatment approaches. Thus, there is a need to fill this gap in knowledge of transport properties of a variety of solutes in the human meniscus.

In this study, we investigate the roles of solute size and tissue structure on diffusion in human meniscus fibrocartilage. We have hypothesized that molecular diffusion is size dependent and anisotropic in these tissues. We will employ our custom fluorescence recovery after photobleaching (FRAP) technique [7, 22, 23] to measure the diffusion coefficient of six different solutes, ranging in size from 332 Da to 150 kDa, in the two principal directions of human meniscus. Such a wide range of molecular weights allows providing a detailed picture of how nutrients (~200Da) and other proteins like growth factors, enzymes, cytokines and extracellular matrix components (from few kDa to over 100kDa) traffic the ECM of the meniscus. Hence, these studies will provide a better understanding of the transport behavior in meniscus tissues, which is crucial for elucidating tissue pathophysiology and for developing new strategies for tissue repair and/or regeneration.

MATERIALS AND METHODS

Molecular probes:

Aimed at providing a detailed picture of how nutrients (~200Da) and larger molecules like growth factors, enzymes, and cytokines (from few hundreds of Da to hundreds of thousands of Da) traffic the ECM of the meniscus, we selected a wide range of molecular probe sizes. Specifically, we measured diffusivity of fluorescein, insulin, bovine serum albumin (BSA), and three dextrans (D3K, D70K and 150kDa), see Table 1 for details.

Specimen preparation:

Samples of meniscal tissue were prepared from nine frozen human menisci obtained from five donors (3 females and 2 males) of age 73.5±6.4 y.o. after autopsy. Menisci were visually inspected to determine their degeneration grade, which was deemed normal to moderately degenerated. Our preliminary studies indicated no statistically significant differences in the values of diffusion coefficients determined in anterior, central or posterior region of the meniscus; therefore, specimens from all the meniscal regions were combined in the same group.

For diffusivity measurements, a corneal trephine was used to punch 5 mm diameter cylindrical specimens in the axial orientation; a compresstome (VF-210–0Z, Precisionary

Instruments, Inc., Natick, MA) was used to cut the specimens to a height of 0.5 mm. For each cylindrical specimen, only one slice was obtained from the deep region of the tissue, far from the superficial or lamellar portions. Similar to our previous studies [7, 24], specimens were confined within two porous plates and a perforated impermeable spacer, and equilibrated overnight in a PBS solution (Sigma-Aldrich Co., St. Louis, MO) containing the molecular probe of interest. Molar concentrations for each solute investigated are reported in Table 1. For each molecule investigated, a total of 9 (n = 9) meniscal samples were tested (one for each meniscus), and a minimum of 3 FRAP tests were performed and averaged on each sample.

For each meniscus, additional tissue blocks were harvested from a meniscal region adjacent to that where specimens for diffusivity measurements were excised. From those tissue blocks, samples were prepared for measurements of water content and for scanning electron microscopy (SEM) imaging of the meniscal collagen structure. A schematic of specimen harvesting and preparation is reported in Figure 1.

Measurement of diffusivity:

A custom FRAP technique, developed in our lab [7], was used to simultaneously measure the diffusion coefficient of solute in the direction parallel (D∥) to and orthogonal ($D^{\perp}$) to the tissue fibers. Experiments were carried out at room temperature (22 °C) using a confocal laser scanning microscope (A1R-SI, Nikon, Japan). The specimens were excited and photobleached by an argon laser (488 *nm* wavelength) using a Plan Apo 20x/0.75 DIC N2 WD 1.0 objective (Nikon, Japan), and emitted fluorescence in the green range of wavelengths. A multi-layer bleaching protocol was used to minimize the error due to the out-of-plane diffusivity contribution [7, 22, 24]. For each test, a time series of 200 video-images of 128×128 pixels (460.7×460.7 μm^2) were collected, including five images prior to bleaching. For fluorescein, insulin, BSA, D3K and D70K, the time lapse between two consecutive images was 0.25s, and that for D150K was 1s. In order to minimize the contribution of the fluorescence emission of the background, pre-bleach images were averaged and then subtracted from the post-bleach image series. The initial bleach spot was a circle of 16 pixels diameter. Images were analyzed using a custom MATLAB-based algorithm [23].

Measurement of water content:

The water content was expressed in terms of water volume fraction (ϕ^w). Specimens were weighed in air (W_{wet}) and in PBS bathing solution (W_s) using the density determination kit together with an analytical balance (Model ML104, Mettler Toledo, Columbus, OH). Specimens were lyophilized overnight and their dry weight (W_{dry}) was measured immediately after lyophilization. Thus, ϕ^w, defined as the ratio of water volume to wet tissue volume, was calculated by [25]:

$$\phi^w = \frac{(W_{wet} - W_{dry})\rho_s}{(W_{wet} - W_s)\rho_w},$$

where ρ_s and ρ_w are the densities of PBS solution and water, respectively.

Imaging of collagen structure:

Axial and circumferential slices obtained from blocks of meniscus tissue were fixed with a 2% glutaraldehyde (Sigma-Aldrich Co., St. Louis, MO) in PBS solution. Samples were then dehydrated in a graded series of ethanol (20%, 50%, 70%, 90%, 100%) and dried by immersion in hexamethyldisilizane (Sigma-Aldrich Co., St. Louis, MO) [26]. The samples were sputter-coated with gold/palladium (Cressington Scientific 108auto Sputter Coater, Redding, CA). High-resolution SEM images were obtained using an Environmental Scanning Electron Microscope (FEI/Phillips XL-30 FEG ESEM, Hillsboro, OR).

Statistical Analysis:

For each solute investigated, a paired t-test was used to determine significant differences in the magnitude of diffusivity along the direction parallel to fibers versus orthogonal to fibers. Also, ANOVA followed by post-hoc Tukey test was used to investigate significant differences in the magnitudes of diffusion coefficients between solutes. A simple linear regression model was used to investigate correlation among solute diffusion coefficients and their Stokes radii (r^s). Additional simple linear regression models were used to investigate correlations among solutes diffusion coefficients and water content in the menisci samples. All the statistical analyses were conducted using Minitab®19 statistical software (Minitab, LLC, State College, PA). For each test conducted, a level of significance of 0.05 ($\alpha = 0.05$) was used. All the data are reported in terms of mean ± standard deviation.

RESULTS

A summary of the measured diffusion coefficients for all the molecular probes investigated in this study is reported in Table 2. The magnitudes of $D^{\parallel}$ and $D^{\perp}$ were significantly different across molecular probes ($p < 0.01$) with those of fluorescein being the largest (106.3±59.6 $\mu m^2/s$ and 56.5±31.6 $\mu m^2/s$, respectively), and those of D150K being the smallest (17.6±12.8 $\mu m^2/s$ and 10.9±8.8 $\mu m^2/s$, respectively). In particular, regression analyses showed a non-linear correlation of the mean relative diffusivity ratios $D^{\parallel}/D_o$ ($R^2 = 0.75$) and $D^{\perp}/D_o$ ($R^2 = 0.74$) (where D_o is the solute diffusivity in water) with the Stokes radii, see Figure 2.

For all the solutes, $D^{\parallel}$ was significantly larger than $D^{\perp}$ ($p < 0.01$). The diffusivity anisotropic ratio (R_D), defined as $R_D = D^{\parallel} / D^{\perp}$, was also calculated, see Figure 3. No statistical differences in the values of R_D were found across molecular probes ($p > 0.05$).

The average value of water content of the menisci samples was 0.70±0.04. No correlations were found between water content and diffusion coefficients, for any solute investigated. However, data suggested a trend of increasing values of diffusion coefficients with the magnitude of the water content (data not shown).

SEM images of meniscal samples showed differences in the organization of the collagen fibers among circumferential and axial sections. Specifically, in circumferential sections the alignment of the collagen fibers allows for the presence of pores that are not apparent in the axial direction, see Figure 4.

DISCUSSION

This study investigates the diffusive transport of molecules and macromolecules in meniscal tissue. To our best knowledge, this is the first contribution reporting measurements of diffusion coefficients in human meniscus.

The diffusion coefficients of fluorescein measured in this study ranged from 56 to 106 $\mu m^2/s$. These results are in agreement with similar diffusivity measurements performed in bovine meniscus (44 to 159 $\mu m^2/s$)[7], and other fibrocartilaginous tissues such as temporomandibular joint (~60 $\mu m^2/s$) [27], and bovine and human annulus fibrosus (from 70 to 180 $\mu m^2/s$) [22, 24]. There are no studies investigating diffusive transport of larger molecules in meniscus. However, the measured values of diffusion coefficients of D3k (25.2 to 39.6 $\mu m^2/s$) and insulin (37 to 57.6 $\mu m^2/s$) are comparable to those of 4kDa fluorescent dextran diffusing in porcine temporomandibular joint (18 to 43 $\mu m^2/s$) [28]. Furthermore, the diffusion coefficients measured for BSA, D70K and D150K were about the half of those reported for similar size molecules diffusing in porcine articular cartilage [29]. The meniscus is significantly less hydrated than articular cartilage and includes, in its organic matter, a significantly higher proportion of collagen fibers [6, 30]. Therefore, it is plausible that the meniscal structure exerts a larger hindrance on diffusing molecules when compared to articular cartilage, resulting in lower solute diffusivities.

Our results indicate that solute diffusivity was significantly affected by solute size, decreasing as the Stokes radius increased, see Figure 2. This is in qualitative agreement with a previous study on diffusivity of various molecular weight fluorescent dextrans in porcine femoral condyle cartilage reporting that diffusion coefficients were inversely related to the molecular radius, following a Stokes-Einstein model [29]. In this study, we found that, when normalized with respect to the values of diffusivity in water D_o, the diffusion coefficients correlated to r^s according to a relationship similar to that proposed by Ogston [31]. This seems appropriate considering that the Stokes-Einstein equation assumes solutes diffusing in a liquid solvent, while Ogston's model describes molecular diffusion in hydrogels, whose structure is similar to that of a soft hydrated cartilaginous tissue.

It was also found that all the solutes investigated in this study presented a similar anisotropic ratio R_D ~2 (Figure 3), which represents an intermediate value with respect to those found in porcine (R_D ~1.5) and bovine (R_D ~3) menisci [7, 8]. These results are further corroborated by several other studies on fibrocartilaginous tissues reporting similar anisotropic ratio [24, 32–37].

The structure and the composition of the meniscal samples were also investigated with the purpose of identifying potential relationships with the measured transport properties. The average water content of the meniscal samples was 70%, which is within the range typically observed for human meniscus [6]. For each solute investigated, no significant correlation of diffusivity with water content was found. However, in agreement with a previous study investigating diffusivity of glucose in porcine meniscus [8], the trend of our data suggest that molecular diffusion coefficients increase with tissue water content. This is also in agreement with most of the theoretical models describing molecular diffusivity in hydrated polymeric

networks increasing with the water volume fraction of the medium [38]. Moreover, SEM images of meniscal sections show presence of pores aligned in the direction of the collagen fibers, see Figure 4. Similar structural organization has already been reported for several other fibrocartilaginous structures, including porcine meniscus [7, 8, 22, 24, 33, 39, 40]. In those studies, it has been hypothesized that the presence of these 'microtubes' may provide justification for the anisotropic behavior of diffusive transport in fibrocartilaginous tissues. That is, solute diffusion is facilitated along the fiber direction since microtubes run parallel to the bundles of collagen fibers; in contrast, in the transversal direction, solute diffusive transport is hindered by the collagen fiber network, as the microtubes appear to be non-contiguous. This hypothesis is supported by our findings showing that, for each molecular solute investigated, $D^{\parallel}$ is about the double of $D^{\perp}$. In addition, this may also explain why all the solutes investigated in this study presented a similar values of R_D: the diameters of the microtubes span from a few to tens of microns (Figure 4), several orders of magnitude larger than the Stokes radius of the largest probe tested (Table 1). Accordingly, all the molecules considered in this study exhibited similar sensitivity to the tissue structure, resulting in similar anisotropic ratios of their diffusivities.

Some limitations of this study are noted. Samples were taken from human menisci obtained during autopsy. As such, a limited range of tissue degenerative states were obtained. In order to better understand how tissue degeneration affects solute transport in meniscus, a larger sample size and range will be investigated in the future. Nonetheless, the use of human tissues in this study provides clinical relevance to these findings. In future studies, we also anticipate examining a wider range of solute sizes, shapes, and net charges, in order to more fully understand solute transport behavior in the tissue.

In summary, the present study represents the first quantitative measurement of diffusivity of an array of molecular solutes ranging from ~300Da to 150KDa in human meniscus. It was found that solute diffusivity is anisotropic, and the magnitude of the diffusion coefficients is inversely related to the Stokes radius of the molecular solutes. The anisotropic diffusivity may be attributed to the orientation of the pores observed in the SEM (i.e., aligned along the direction of the collagen fibers in the tissue), suggesting a preferred pathway for circumferential diffusion. Water content of the tissue was not significantly correlated to solute diffusivity. These findings are crucial for better understanding of transport properties in meniscal tissues, as well as for the future development of numerical models on meniscus homeostasis.

ACKNOWLEDGMENTS

The authors wish to thank the Ultramicroscopy Center at the University of Miami Miller School of Medicine for use of the confocal microscope for this study, Dr. Loren Latta and Abeer Albarghouthi for their assistance in tissue harvesting, and Julian Milberg for his assistance in SEM imaging. The project described was supported by Grant Number 1R01AR073222 from the NIH (NIAMS). The authors have nothing to disclose.

REFERENCES

1. Shrive NG, O'Connor JJ, Goodfellow JW. Load-bearing in the knee joint. Clinical orthopaedics and related research 1978; 131: 279–287.

2. Murphy L, Helmick CG. The impact of osteoarthritis in the United States: a population-health perspective. AJN The American Journal of Nursing 2012; 112: S13–S19. [PubMed: 22373741]

3. Englund M, Haugen IK, Guermazi A, Roemer FW, Niu J, Neogi T, et al. Evidence that meniscus damage may be a component of osteoarthritis: the Framingham study. Osteoarthritis and Cartilage 2016; 24: 270–273. [PubMed: 26318660]

4. Greis PE, Bardana DD, Holmstrom MC, Burks RT. Meniscal injury: I. Basic science and evaluation. JAAOS-Journal of the American Academy of Orthopaedic Surgeons 2002; 10: 168–176.

5. Arnoczky SP, Warren RF. Microvasculature of the human meniscus. The American journal of sports medicine 1982; 10: 90–95. [PubMed: 7081532]

6. Athanasiou KA, Sanchez-Adams J. Engineering the knee meniscus. Synthesis Lectures on Tissue EngineerinG 2009; 1: 1–97.

7. Travascio F, Zhao W, Gu WY. Characterization of anisotropic diffusion tensor of solute in tissue by video-FRAP imaging technique. Annals of biomedical engineering 2009; 37: 816.

8. Kleinhans KL, Jaworski LM, Schneiderbauer MM, Jackson AR. Effect of static compressive strain, anisotropy, and tissue region on the diffusion of glucose in meniscus fibrocartilage. Journal of biomechanical engineering 2015; 137: 101004. [PubMed: 26201748]

9. Jackson AR, Gu WY. Transport properties of cartilaginous tissues. Current rheumatology reviews 2009; 5: 40–50. [PubMed: 20126303]

10. Makris EA, Hadidi P, Athanasiou KA. The knee meniscus: structure–function, pathophysiology, current repair techniques, and prospects for regeneration. Biomaterials 2011; 32: 7411–7431. [PubMed: 21764438]

11. Fithian DC, Kelly MA, Mow VC. Material properties and structure-function relationships in the menisci. Clinical orthopaedics and related research 1990; 252: 19–31.

12. Proctor CS, Schmidt MB, Whipple RR, Kelly MA, Mow VC. Material properties of the normal medial bovine meniscus. Journal of orthopaedic research 1989; 7: 771–826. [PubMed: 2677284]

13. Nguyen AM, Levenston ME. Comparison of Osmotic Swelling Influences on Meniscal Fibrocartilage and Articular Cartilage Tissue Mechanics in Compression and Shear. Journal of orthopaedic research 2012; 30: 98–102.

14. Sweigart MA, Zhu CF, Burt DM, DeHoll PD, Agrawal CM, Clanton TO, et al. Intraspecies and interspecies comparison of the compressive properties of the medial meniscus. Annals of Biomedical Engineering 2004; 32: 1569–1579. [PubMed: 15636116]

15. Gabrion A, Aimedieu P, Laya Z, Havet E, Mertl P, Grebe R, et al. Relationship between ultrastructure and biomechanical properties of the knee meniscus. Surgical and Radiologic Anatomy 2005; 27: 507–510. [PubMed: 16308664]

16. Tissakht M, Ahmed AM. Tensile stress-strain characteristics of the human meniscal material. Journal of biomechanics 1995; 28: 411–422. [PubMed: 7738050]

17. Chia HN, Hull ML. Compressive moduli of the human medial meniscus in the axial and radial directions at equilibrium and at a physiological strain rate. Journal of orthopaedic research 2008; 26: 951–956. [PubMed: 18271010]

18. Leslie BW, Gardner DL, McGeough JA, Moran RS. Anisotropic response of the human knee joint meniscus to unconfined compression. Proceedings of the Institution of Mechanical Engineers, Part H: Journal of Engineering in Medicine 2000; 214: 631–635.

19. Skaggs DL, Warden WH, Mow VC. Radial tie fibers influence the tensile properties of the bovine medial meniscus. Journal of Orthopaedic Research 1994; 12: 176–185. [PubMed: 8164089]

20. Spilker RL, Donzelli PS, Mow VC. A transversely isotropic biphasic finite element model of the meniscus. Journal of biomechanics 1992; 25: 1027–1045. [PubMed: 1517263]

21. Sanchez-Adams J, Willard VP, Athanasiou KA. Regional variation in the mechanical role of knee meniscus glycosaminoglycans. Journal of applied physiology 2011; 111: 1590–1596. [PubMed: 21903884]

22. Travascio F, Gu WY. Anisotropic diffusive transport in annulus fibrosus: experimental determination of the diffusion tensor by FRAP technique. Annals of biomedical engineering 2007; 35: 1739–1748. [PubMed: 17605108]

23. Travascio F, Gu WY. Simultaneous measurement of anisotropic solute diffusivity and binding reaction rates in biological tissues by FRAP. Annals of biomedical engineering 2011; 39: 53–65. [PubMed: 20686922]
24. Travascio F, Jackson AR, Brown MD, Gu WY. Relationship between solute transport properties and tissue morphology in human annulus fibrosus. Journal of Orthopaedic Research 2009; 27: 1625–1630. [PubMed: 19489044]
25. Jackson A, Yao H, Brown MD, Gu WY. Anisotropic ion diffusivity in intervertebral disc: an electrical conductivity approach. Spine 2006; 31: 2793–2789.
26. Hayat MA. Glutaraldehyde: role in electron microscopy. Micron and Microscopica Acta 1986; 17: 115–135.
27. Shi C, Wright GJ, Ex-Lubeskie CL, Bradshaw AD, Yao H. Relationship between anisotropic diffusion properties and tissue morphology in porcine TMJ disc. Osteoarthritis and cartilage 2013; 21: 625–633. [PubMed: 23353670]
28. Shi C, Kuo J, Bell PD, Yao H. Anisotropic solute diffusion tensor in porcine TMJ discs measured by FRAP with spatial Fourier analysis. Annals of Biomedical Engineering 2010; 38: 3398–3408. [PubMed: 20582475]
29. Leddy HA, Guilak F. Site-specific molecular diffusion in articular cartilage measured using fluorescence recovery after photobleaching. Annals of biomedical engineering 2003; 31: 753–760. [PubMed: 12971608]
30. Sophia Fox AJ, Bedi A, Rodeo SA. The basic science of articular cartilage: structure, composition, and function. Sports health 2009; 1: 461–468. [PubMed: 23015907]
31. Ogston AG, Preston BN, Wells JD. On the transport of compact particles through solutions of chain-polymers. . Proceedings of the Royal Society of London. A. Mathematical and Physical Sciences 1973; 333: 297–316.
32. Leddy HA, Haider MA, Guilak F. Diffusional anisotropy in collagenous tissues: fluorescence imaging of continuous point photobleaching. Biophysical journal 2006; 91: 311–316. [PubMed: 16603503]
33. Jackson AR, Yuan TY, Huang CY, Travascio F, Gu WY. Effect of compression and anisotropy on the diffusion of glucose in annulus fibrosus. Spine 2008; 33: 1. [PubMed: 18165741]
34. Hsu EW, Setton LA. Diffusion tensor microscopy of the intervertebral disc anulus fibrosus. Magnetic Resonance in Medicine. An Official Journal of the International Society for Magnetic Resonance in Medicine 1999; 41: 992–999.
35. Filidoro L, Dietrich O, Weber J, Rauch E, Oerther T, Wick M, et al. High-resolution diffusion tensor imaging of human patellar cartilage: feasibility and preliminary findings. Magnetic Resonance in Medicine:: An Official Journal of the International Society for Magnetic Resonance in Medicine 2005; 53: 993–998.
36. Meder R, De Visser SK, Bowden JC, Bostrom T, Pope JM. Diffusion tensor imaging of articular cartilage as a measure of tissue microstructure. Osteoarthritis and Cartilage 2006; 14: 875–881. [PubMed: 16635581]
37. De Visser SK, Crawford RW, Pope JM. Structural adaptations in compressed articular cartilage measured by diffusion tensor imaging. Osteoarthritis and Cartilage 2008; 16: 83–89. [PubMed: 17625926]
38. Amsden B Solute diffusion within hydrogels. Mechanisms and models. Macromolecules 1998; 31: 8382–8395.
39. Jackson AR, Travascio F, Gu WY. Effect of mechanical loading on electrical conductivity in human intervertebral disk. Journal of biomechanical engineering 2009; 131: 054505. [PubMed: 19388789]
40. Iatridis JC, ap Gwynn I. Mechanisms for mechanical damage in the intervertebral disc annulus fibrosus. Journal of biomechanics 2004; 37: 1165–1175. [PubMed: 15212921]
41. Mustafa MB, Tipton DL, Barkley MD, Russo PS, Blum FD. Dye diffusion in isotropic and liquid-crystalline aqueous (hydroxypropyl) cellulose. Macromolecules 1993; 26: 370–378.
42. Yousefi R, Taheri B, Alavi P, Shahsavani MB, Asadi Z, Ghahramani M, et al. Aspirin-mediated acetylation induces structural alteration and aggregation of bovine pancreatic insulin. Journal of Biomolecular Structure and Dynamics 2016; 34: 362–375. [PubMed: 25994118]

43. Axelsson I Characterization of proteins and other macromolecules by agarose gel chromatography. Journal of Chromatography A 1978; 152: 21–32.

44. Sigma. Fluorescein Isorhiocyanate-Dextran. Product Information 1997: 1–3.

45. Culbertson CT, Jacobson SC, Ramsey JM. Diffusion coefficient measurements in microfluidic devices. Talanta 2002; 56: 365–373. [PubMed: 18968508]

46. Vogel S Life's devices: the physical world of animals and plants, Princeton University Press 1988.

47. Gaigalas AK, Hubbard JB, McCurley M, Woo S. Diffusion of bovine serum albumin in aqueous solutions. The Journal of Physical Chemistry 1992; 96: 2355–2359.

48. Arrio-Dupont M, Cribier S, Foucault G, Devaux PF, d'Albis A. Diffusion of fluorescently labeled macromolecules in cultured muscle cells. Biophysical journal 1996; 70: 2327–2332. [PubMed: 9172756]

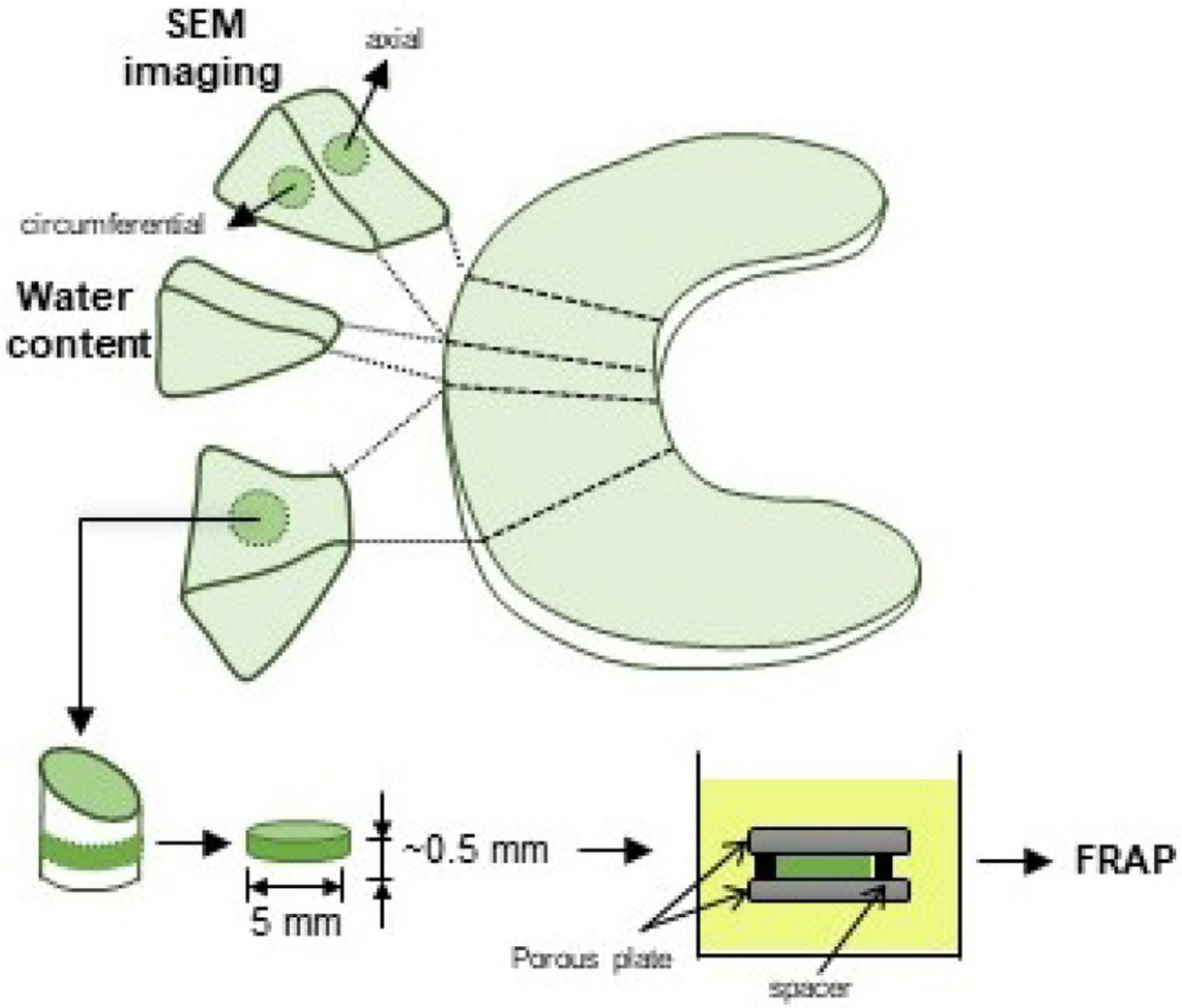

Figure 1:

Schematic of specimen preparation. Location and size of the specimens is shown. For FRAP tests, cylindrical specimens with a height of 0.5 mm and a diameter of 6 mm were prepared from the central region of the meniscus along the axial direction. For SEM imaging, specimens were prepared from central regions along the axial and the circumferential directions.

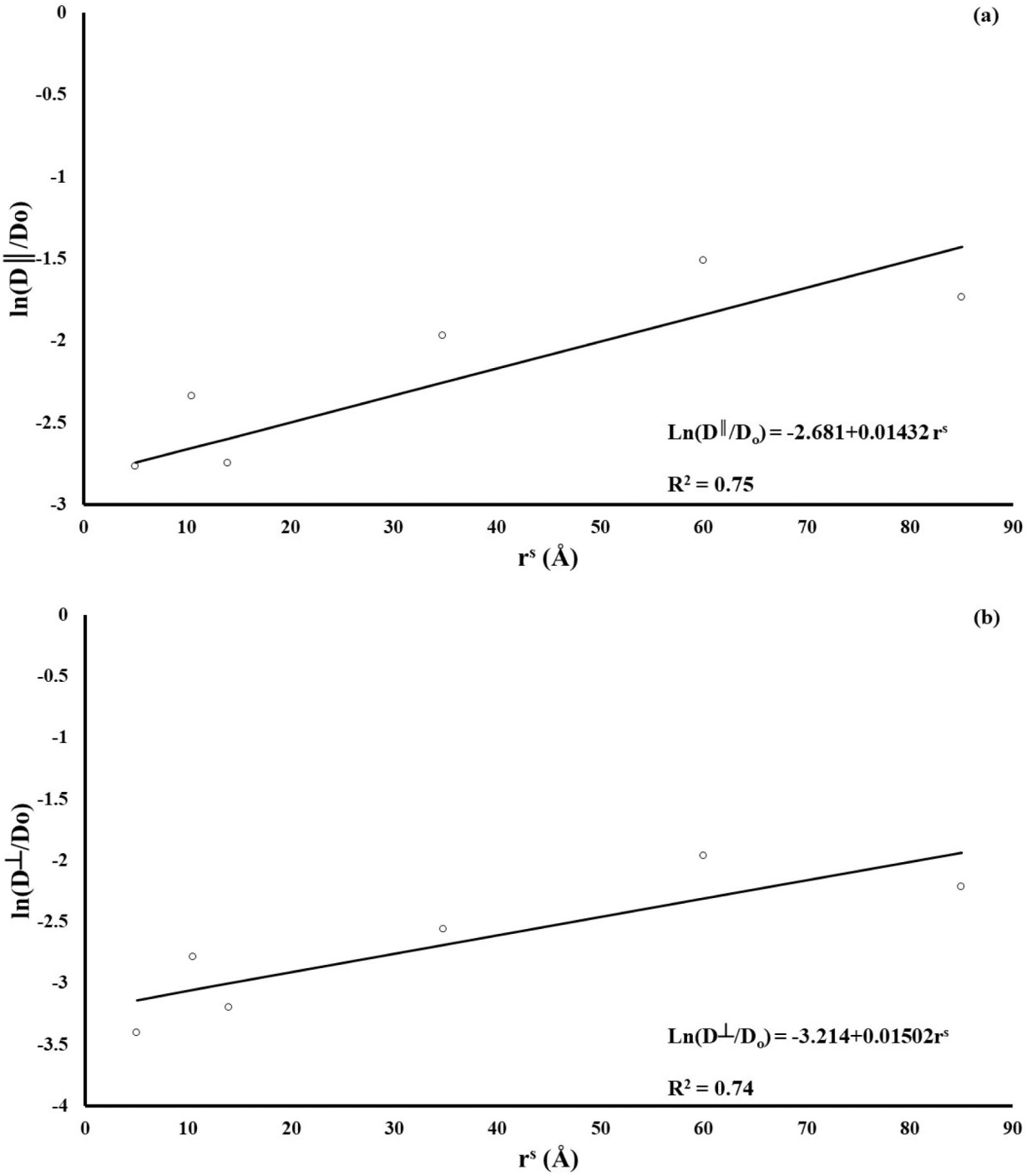

Figure 2:

Diffusivity is inversely related to solute size. (a) solute diffusivity along tissue fiber direction ($D^{\parallel}$); (b) solute diffusivity in the direction orthogonal to tissue fibers ($D^{\perp}$). For all the cases reported, diffusion coefficients have been normalized with respect to solute diffusivity in water (D_o).

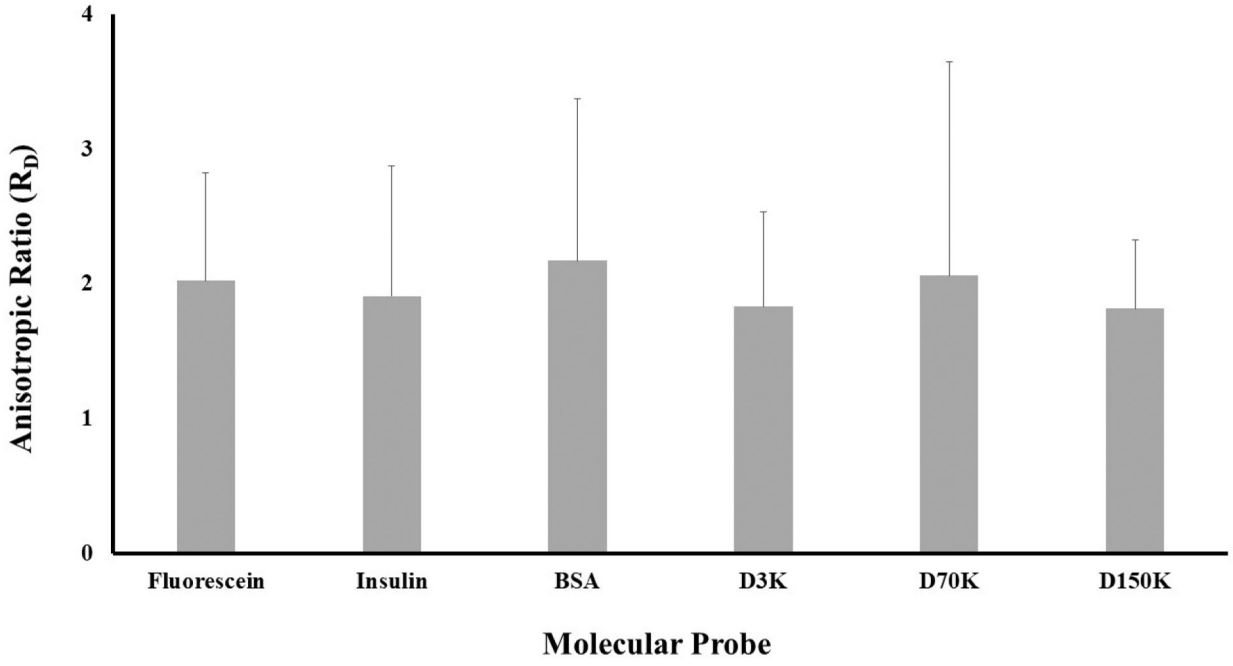

Figure 3:

Solute diffusivity in meniscus is anisotropic. For all the solutes investigated, the diffusivity anisotropic ratio, defined as $R_D = D^{\parallel} / D^{\perp}$, is reported.

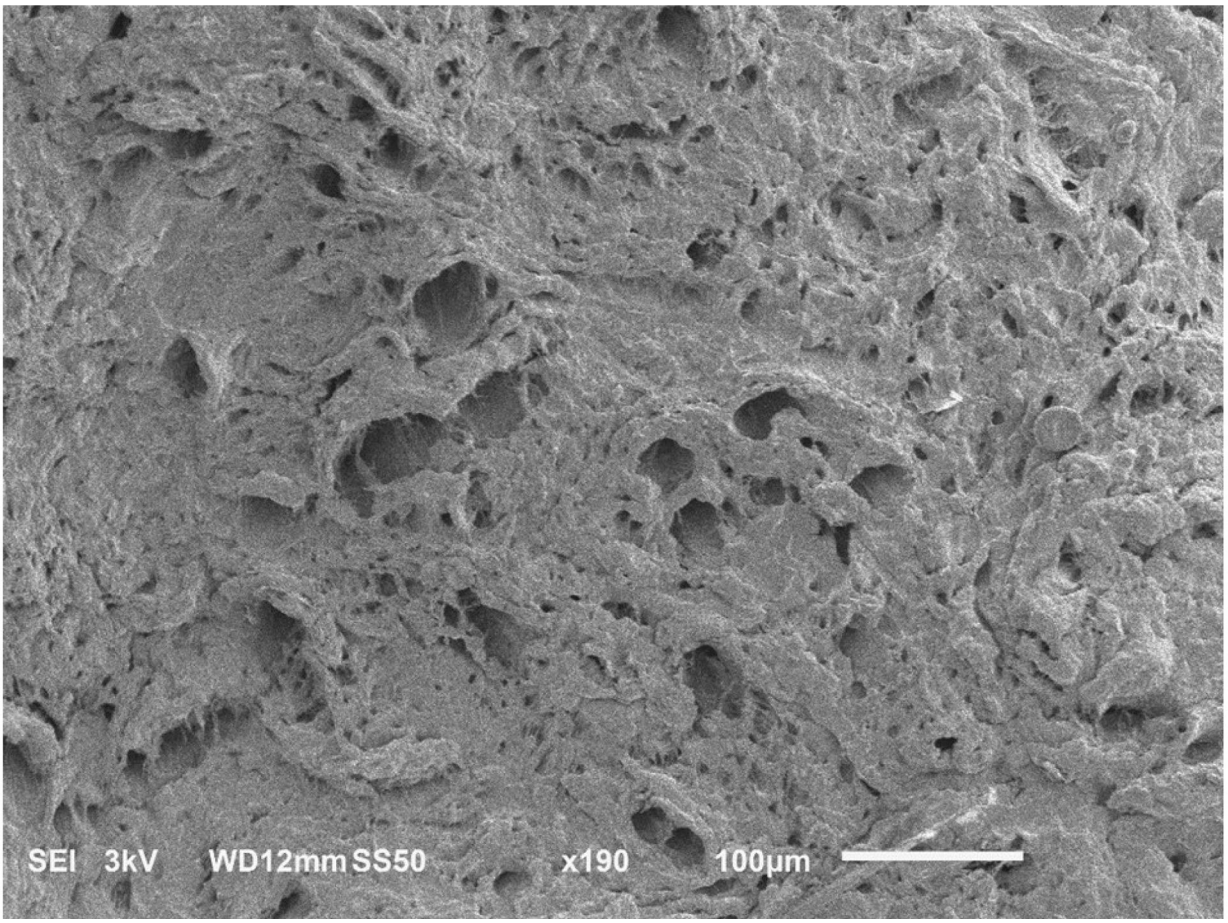

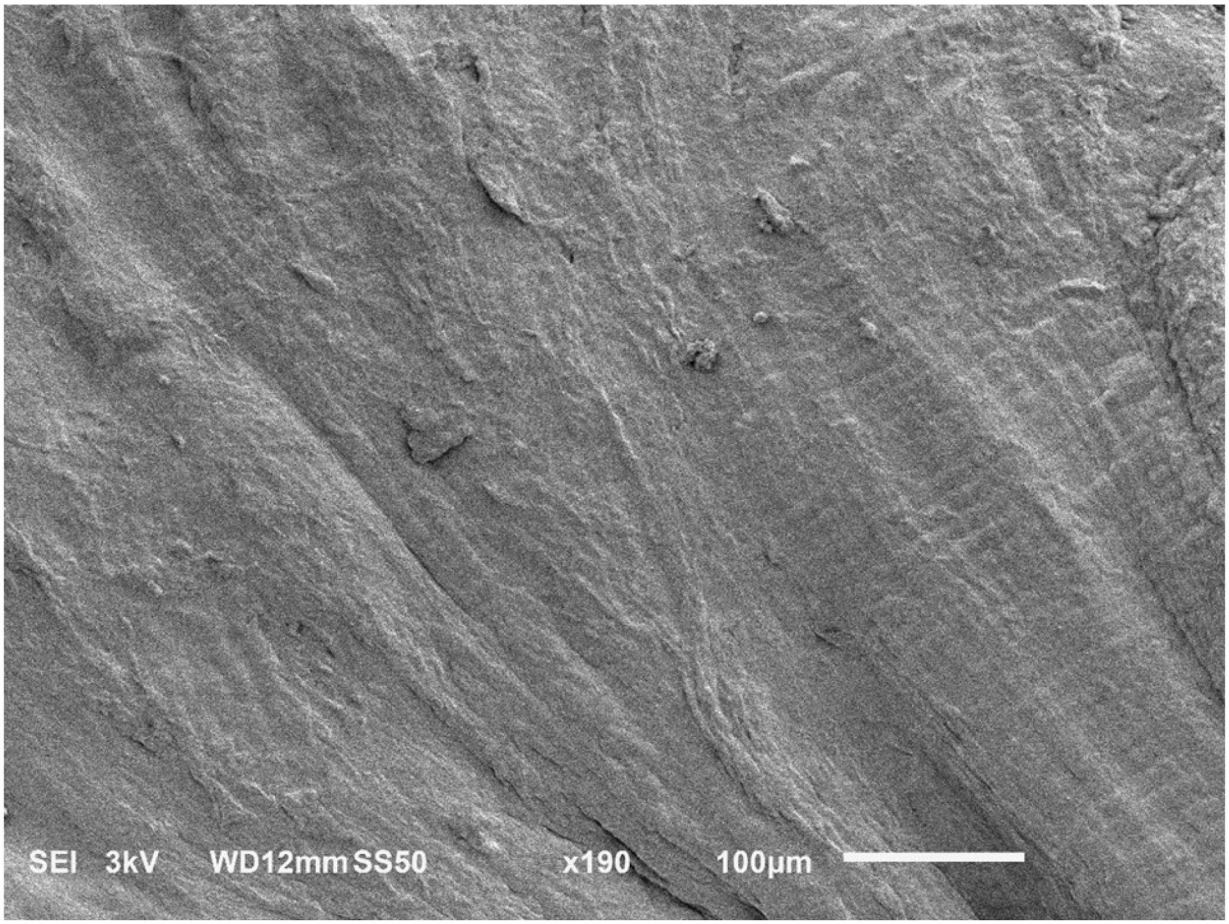

Figure 4:
SEM images of human meniscus showing unique collagen architecture. (a) circumferential section showing presence of pores aligned in the direction of the collagen fibers; (b) axial section, no pores are visible.

Table 1.

Summary of molecular probes used in this study.

Molecule	Source	Abbreviation	MW [Da]	r^s(Å)	D_0 [μm²/s]	Concentration in PBS [M]
Fluorescein	Sigma-Aldrich	Fluorescein	332	5.02[a]	425[e]	10^{-4}
Insulin-FITC labeled human	Sigma-Aldrich	Insulin	5,807	10.5[b]	150[f]	4.3×10^{-5}
Albumin from Bovine Serum (BSA), Alexa Fluor™ 488 conjugate	Molecular Probes	BSA	66,000	34.8[c]	63[g]	3.8×10^{-6}
Dextran, Fluorescein, 3000 MW	Molecular Probes	D3K	3,000	14[d]	155[h]	1.7×10^{-4}
Dextran, Fluorescein, 70000 MW	Molecular Probes	D70K	70,000	60[d]	30[h]	1.8×10^{-5}
Fluorescein isothiocyanate-dextran 150000 MW	Sigma-Aldrich	D150K	150,000	85[d]	25[h]	3.3×10^{-5}

[a] [41];

[b] [42];

[c] [43];

[d] [44];

[e] [45];

[f] [46];

[g] [47];

[h] [48]

Table 2.

Summary of molecular probes diffusivities. Data are reported in terms of mean ± standard deviation. Grouping of pairwise comparison obtained after Tukey test are reported.

Molecular Probe	$D_{\parallel}$ [$\mu m^2/s$]	Grouping	$D^{\perp}$ [$\mu m^2/s$]	Grouping
Fluorescein	106.3±59.6	A	56.5±31.6	A
Insulin	57.6±57.6	BC	37±11.4	BC
BSA	35.1±22.4	BC	19.4±13.6	BC
D3K	39.6±21.2	B	25.2±18	AB
D70K	26.5±5.2	BC	16.8±7.2	BC
D150K	17.6±12.8	C	10.9±8.8	C